Calibration of the velocity scale

September 28, 2017

Contents

1 Introduction

The calibration of the velocity scale of the Mossbauer spectrum is a prerequisite for a reliable evaluation of the experimental spectra, especially concerning line positions and their widths. The standard method is the determination of the line positions of an α-iron absorber on the channel scale and calculating the mm/s per channel by the known overall splitting of the iron absorber or the average of the three splittings (1,6),(2,5) and (3,4). The Fit;o)- Mössbauer spectrum fitting program takes the unfolded spectrum and the appropiate average of the 12 absorption lines [1]. In WMOSS4 [2] a simple interpolation by the best straight line fitted to the peak positions is offered. The fit-program NORMOS [3] interpolates using a cubic spline between the first and the last velocity value. Other programs [4, 5, 6, 7, 8, 9, 10] do not handle the non-linearity of the velocity scale. The fit of the calibration spectrum stops at some local minimum where the position of the more intense absorption lines (1 and 6 in case of $\alpha{-}Fe$) have the higher weight for the scaling factor.
The linearity error for driving units in the triangular mode is guaranteed to be $< 0.15\%$ at the resonance frequency by WISSEL [11], which still corresponds to more than one channel in 10^3. Using optimal soft springs an error less than 0.5% can be promised by FASTCOMTEX [12].

A more accurate calibration of the velocity scale of a Mössbauer spectrum can only be obtained with a more elaborate correction function for the non-linearity of the driving unit. Several functions based on a Fourier expansion are constructed to get a fit over a large velocity range to both halfs of the MCS-spectrum.

2 Theoretical considerations

2.1 Velocity correction function

The fourier series of the triangular wave v(t) on the time axis

$$v(t) = -v_{max}\frac{4}{\pi^2}\left(cos\,\omega t + \frac{cos\,3\omega t}{3^2} + \frac{cos\,5\omega t}{5^2} + ...\right) \tag{1}$$

is to some accuracy reproduced by the signal of the function generator driving the transducer. The deviations from the triangular wave form may be caused by deviations δa_i from the amplitudes $1/(2i+1)^2$ at frequencies $\omega_i = (2i+1)\omega$ of the components of the series. In that case the function

$$dv(k) = \sum_i \delta a_i\, cos\,(\omega_i k) \tag{2}$$

should be a good choice for correcting the velocity scale. The continous variable t is replaced by the channel number k corresponding to time steps Δt such that

$$\begin{aligned} v(k) + dv(k) &= -v_{max}\frac{4}{\pi^2}\left(cos\,\Omega * k + \frac{cos\,3\Omega k}{3^2} + \frac{cos\,5\Omega k}{5^2} + ...\right) \\ \Omega &= \frac{\pi}{2}\,/\,channel(v=0) \end{aligned} \tag{3}$$

is supposed to be the correct velocity to channel conversion.
However, more successfully turned out taking all frequencies $\Omega_i = i\Omega$ (i=1,2,...). The cos functions implies a symmetry which is broken by adding sin functions such that

$$dv(k) = \sum_i \delta a_i\, cos\,(\Omega_i k) + \delta b_i\, sin\,(\Omega_i k) \tag{4}$$

These two correction equations 2 and 4 allow for 4 cases using the different frequency sets $\Omega_i = i\Omega$ and $\Omega_i = (2i+1)\Omega$. Two further cases are introduced by changing the sign of the amplitudes δb_i for channels k of the second half of the spectrum. Up to 18 parameters can be declared. The summation index runs from 1-9 in case of two amplitudes $\delta a_i, \delta b_i$.
The sinusiodal mode is also not free from nonlinearities of the velocity scale and can be corrected by the same functions. The amplitudes δa_i,δb_i turn out to be very small.

2.2 Interpolation of the theory function

The velocity scale of the theory is different from the velocity scale attached to the channels. The velocity steps $\Delta v_t = v_{tj+1} - v_{tj}$ of the theory are choosen to be larger than $4 * v_{max}/N$, with the number of channels N of the full period. Such a choice saves computation time since the number of theory points $N_t = 2*v_{max}/\Delta v_t$ is the number of time consuming convolution integrals. The selection of the 4 equidistant theory points $v_{tj-1}, ..., v_{tj+2}$ is displayed in Fig.1. The velocity v_{i+3} attached to channel i+3 is as close as possible to v_{tj} or v_{tj+1}, the two velocities with the exact theory values th_j and th_{j+1}. The first and last sampling points are only approximated by the 3 constants of a parabola.

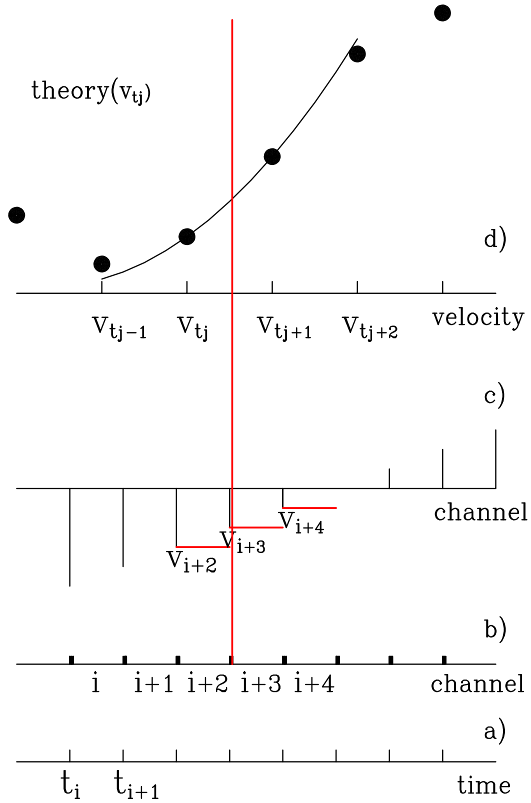

Figure 1: a) the time t with time markers t_i at the begin of channel i in b). The dwell time of the channels $t_{i+1}-t_i$ is reduced by the dead time for the channel switch from i to i+1 (indicated by the thick bars). c) The velocities at the beginning of the channels are represented by bars pointing downwards ($v < 0$), crossing v=0 and upwards ($v > 0$). A stepwise velocity increase is depicted by the horizontal red lines. The theoretical spectrum is shown in d). It has its own velocity scale v_{tj}. At v_{i+3} the function value is interpolated by a parabola calculated from v_{tj-1} until v_{tj+2}. The scale of c) is adjusted to the best fit of the interpolated values with the experimental spectrum.

The parabola $th = av^2 + bv + c$ is fitted to the theory curve at the four equidistant v-values replaced by Δv_t units ($(v - v_j)/\Delta v_t = -1, 0, 1, 2$) so that the linear equation system reads:

$$\begin{aligned} th_{j-1} &= a - b + c \\ th_j &= c \\ th_{j+1} &= a + b + c \\ th_{j+2} &= 4a + 2b + c \end{aligned} \tag{5}$$

The constants b and c can be expressed by a. $f(a)$ is minimized so that the parabola hits the two inner points (j) and (j+1) and approximates the outer points (j-1) and

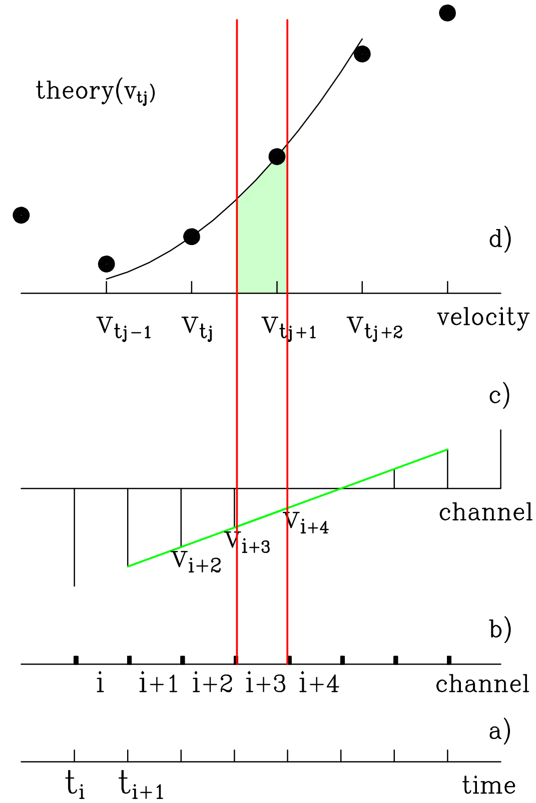

Figure 2: For a) and b) see Fig.1. c) The velocity changes linearily from v_{i+3} to v_{i+4} by a constant accelleration. d) The theoretical spectrum is integrated from the interpolated values at v_{i+3} to v_{i+4}.

(j+2). The following set of equations determine a,b and c.

$$\begin{aligned}
b &= th_{j+1} - th_j - a \\
c &= th_j \\
f(a) &= (th_{j-1} - (a - b + c))^2 + (th_{j+2} - (4a + 2b + c))^2 \\
\frac{\partial f}{\partial a} &= 0 \\
=> a &= \frac{1}{4}(th_{j+2} + th_{j-1} + th_{j+1} - 3th_j)
\end{aligned} \tag{6}$$

Following Oshtrakha and Semionkin [13] the velocity is constant for the dwell time of a channel and is accelerated in a very short time preferably during the daedtime for switching to the next channel (see Fig. 1). If this is the case, the theoretical value assigned to channel i+3 is the intersection of the red straight line with the theory curve. In Fig. 2 the velocity is linearly increasing from v_{i+3} to v_{i+4} during the time t_{i+3} till $t_{i+4} = t_{i+3} + \Delta t$. The integral from t_{i+3} till $t_{i+3} + \Delta t$ under the theoretical curve devided by Δt corresponds to the counts collected in channel i+3.

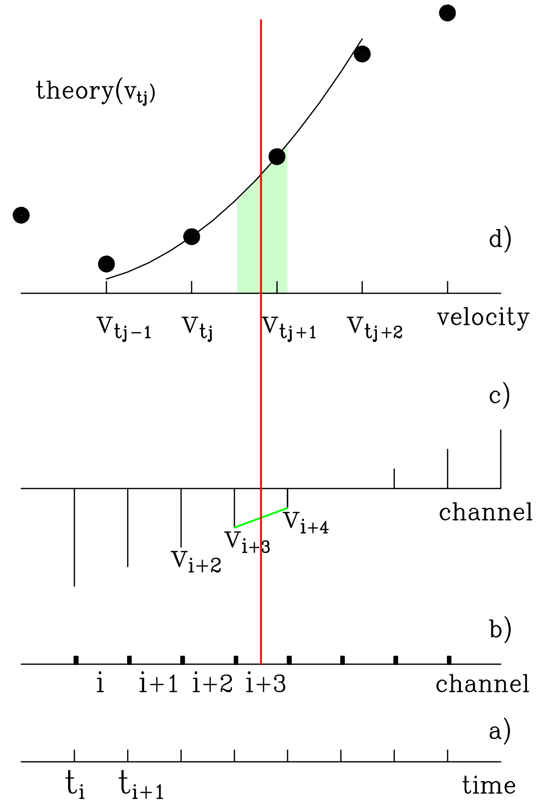

Figure 3: For a) and b) see Fig.1. c) The velocity change linearly. d) The theoretical spectrum is interpolated at $(v_{i+3} + v_{i+4})/2$.

$$
\begin{aligned}
I_{th} &= \frac{1}{\Delta t} \int_{t_{i+3}}^{t_{i+4}} th(v(t))dt \qquad (7) \\
I_{th} &= \frac{1}{\Delta t} \int_{t_{i+3}}^{t_{i+4}} th(v(t)) \frac{dt}{dv} dv
\end{aligned}
$$

With the constant acceleration dv/dt and $dv/dt \cdot \Delta t = \Delta v = v_{i+4} - v_{i+3}$ the integral

$$
\begin{aligned}
I_{th} &= \frac{1}{\Delta v} \int_{t_{i+3}}^{t_{i+4}} th(v)dv \qquad (8) \\
&= \frac{1}{\Delta v} \left[\frac{1}{3} a v^3 + \frac{1}{2} b v^2 + cv \right]_{t_{i+3}}^{t_{i+4}} \\
&= \frac{1}{3} a (v_{i+3}^2 + v_{i+4}^2 + v_{i+3} \cdot v_{i+4}) + \frac{1}{2} b (v_{i+3} + v_{i+4}) + c
\end{aligned}
$$

is the theoretical value of channel i+3. A linear interpolation is sufficient for small velocity steps achieved by large channel numbers. Omitting the constant a (a=0) the integral is given by

$$I_{th} = \frac{1}{2}b(v_{i+3} + v_{i+4}) + c \qquad (9)$$
$$= \frac{1}{2}(v_{i+3} + v_{i+4})(th_{j+1} - th_j) + th_j$$

Only two values of the theory have to be calculated. The integral can also be well approximated by the theory value at the center of channel i+3 at $\frac{1}{2}(v_{i+3}+v_{i+4})$ multiplied by $\Delta v = v_{i+4} - v_{i+3}$ as is obvious from Fig. 3. The disadvantage is the recalculation of the theory at the center of the channels scaled by velocity and not by the time. The majority of the Mossbauer programs have only this possibility. It shall be noted that the intuitiv choice of the center of the channel implicates a constant acceleration. The stepwise increase of the velocity as shown in Fig. 1 seems to be not realized in any of the programs.

3 How to calibrate

The calibration of the velocity to channel scale in principle is determined by two parameters, the maximum velocity $v_{max}[mm/s]$ or $\alpha[mm/s/channel]$ and the channel of zero velocity k_{v0} or the folding point $k_{v0} + N/4$. These two values are obtained by a fit of the positions of 6 independend lines of the $\alpha - iron$ spectrum of one of the half-period spectra.

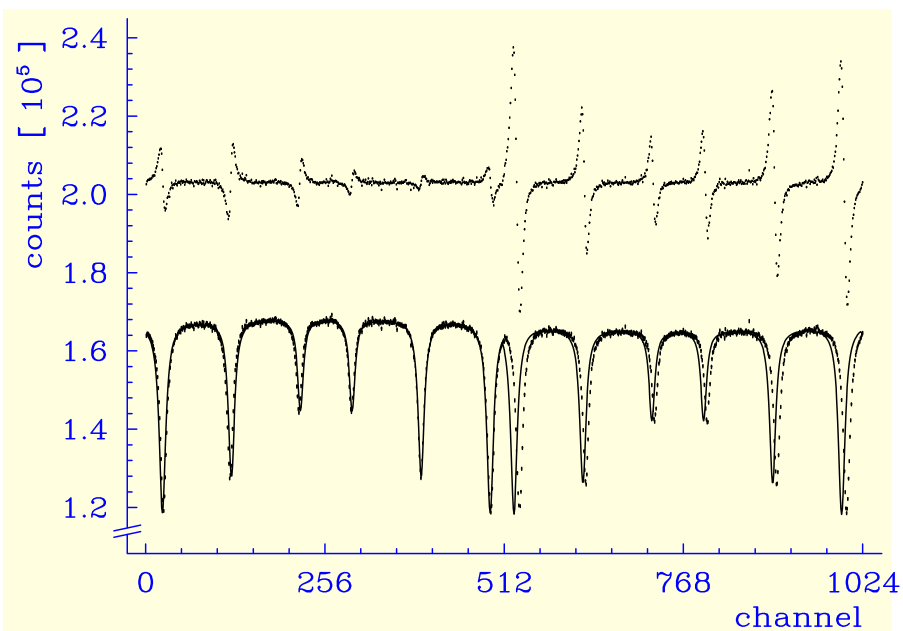

Figure 4: Calibration spectrum with $v_{max} \approx 6mm/s$ for quadrupole split Fe^{2+}-spectra. The α-iron foil of a thickness of 10μ was mounted at 45^o such that the thickness becomes $\sqrt{2} \cdot 10\mu$.

The separation of $\Delta_{1,6} = 10.64256mm/s$ devided by the difference $ch_{1,6}$ between channels of lines 1 and 6 gives $\alpha[mm/s/channel]$ and times N/4 the maximum velocity

$v_{max}[mm/s]$. The zero velocity channel is obtained from the isomer shift is (referred to the source).

$$k_{v0} = \frac{1}{2}(ch_1 + ch_6) + is \cdot \alpha$$

If nonlinearity corrections dv_i are not necessary the full period spectrum should fit with the line positions.

$$\begin{aligned} p_1 &= -5.32128 + is, \quad p_2 = -3.08079 + is, \quad p_3 = -0.84029 + is \\ p_6 &= 5.32128 + is, \quad p_5 = 3.08079 + is, \quad p_4 = 0.84029 + is \end{aligned} \tag{10}$$

Typically the velocity scale is nonlinear indicated by large χ^2-value imposing the positions of Eq. 10 by the Hamiltonian with an internal field of 33.05 Tesla and an isomershift (here ^{57}Co/Rh-source) of -0.114mm/s. In Fig. 4 the left half is fitted . The nonlinearity is obvious by the large misfit of the first and second line. The fitted pa-

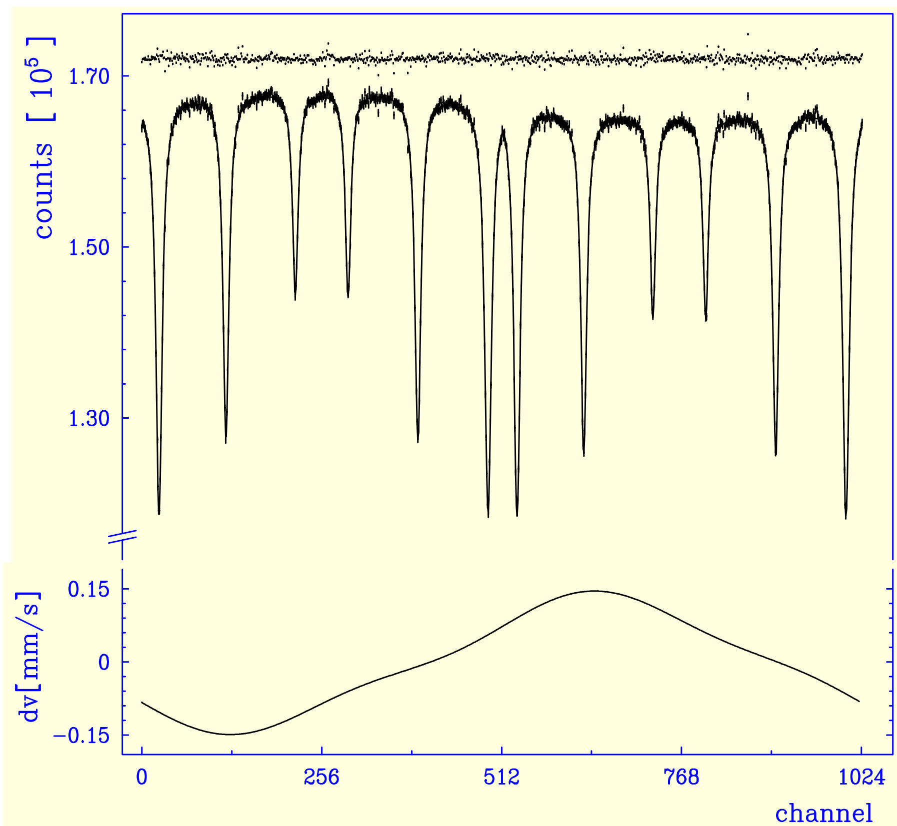

Figure 5: Calibration spectrum fitted with 6 nonlinearity parameter ($chi^2 = 1.040$). The correction of the velocity dv at each channel from equidistant values $4v_{max}/1024$ varies from -0.15mm/s to +0.15mm/s which is almost the linewiths of $2\Gamma_n$ of the absorption lines.

rameters are $v_{max} = 5.831$ and $k_{v0} = 253.50$ with $\chi^2 = 33$. The fit with 6 nonlinearity parameter gives a $\chi^2 = 1.026$ and a slightly larger $v_{max} = 5.864$. The folding point $k_{v0} + N/4 = 512.08$ shifts to a value almost N/2 and is also very close to the folding point 512.50 obtained by the standard procedure described in [4].

The misfit of the right half of the spectrum is much larger. The theory appears to be shifted to the left. The fit including the second half of the full period spectrum shown in Fig. 5 reaches $\chi^2 = 1.040$ and changes again the maximum velocity to $v_{max} = 5.918$ and the folding point by 2 channels to $k_{v0} + N/4 = 514.60$.

The fit is obtained without any line broadening of the transitions in the α-iron foil. The intensity ratio of lines (2,5)/(3,4)=2 for random oriented internal fields changes to 2.128 and the thickness of the foil comes out to be $10.62\mu m$ which is somewhat lager than the nominal value of $10\mu m$. The 5mCi-source has a slightly reduced Lamb-Mössbauer factor $f_{source} = 0.73$ instead of 0.75 and a Voigt-profile with $\sigma_{Gauss} = 0.47\Gamma_N$ and $\Gamma = 1.05 \cdot \Gamma_N$. Fitting the Voigtprofile with a Lorentzian shape the width $\Gamma = 0.119mm/s$ is without doubt too large to be caused by selfabsorption effects of an old 5mCi-source. The equipment of this measurement was not of high quality as obvious by the large nonlinearity correction so that apparative broadening independent on the velocity compensates a small extra boadening of the source width.

References

[1] Jari Hjollum and Morten Bo Madsen, **Fit;o)** - A Mössbauer spectrum fitting program, Earth and Planetary Physics, Juliane Maries vej 30, Niels Bohr Institute, University of Copenhagen, Denmark, 2009.

[2] Thomas A. Kent and Ion Prisecaru, Program **WMOSS4**, url = http://www.wmoss.org, 2013.

[3] R. N. Brand, Program **NORMOS**, url = http://www.wissel-gmbh.de, 2006.

[4] Z. Klencsár, Program **MOSSWINN**, url = http://www.mosswinn.com, 2014.

[5] Szilárd Sajti, Program **FitSuite**, url = http://www.fs.kfki.hu, 2009.

[6] Sirko Kamusell, Program **Moessfit**, url = http://www.tu-dresden.de/die tu dresden/fakultaeten/ fakultaet mathematik und naturwissenschaften/ fachrichtung physik/ifp/mitarbeiter ifp/mitarbeiter details/Moessfit, 2014.

[7] Tomáš Žák, Program **CONFIT2000** Mssbauer spectra fitting, url=http://www.ipm.cz/group/emp/confita.html, 2017.

[8] Lukasz Duraj and Krzysztof Ruebenbauer, Program **Mosgraf**-2009: The Mssbauer data processing suite of applications, NUKLEONIKA 58,16-16 (2013), 2013.

[9] Ken Lagarec and Denis G Rancourt, Program **Recoil**- Mössbauer Spectral Analysis Software for Windows, url =http://www.academia.edu/1072429/Recoil-Mössbauer_Spectral_Analysis_Software_for_Windows, 1999.

[10] Kristjan Jonsson, Program **Mfit** : A Program For Fitting Mssbauer Spectra, url=https://notendur.hi.is/kj/mfit, 1999.

[11] info@wissel.eu, WissEl - Wissenschaftliche Elektronik GmbH, url=http://www.wissel-instruments.de, 2017.

[12] info@fastcomtec.com, FAST ComTec Communication Technology GmbH, url=https://www.fastcomtec.com/, 2017.

[13] Michael I. Oshtrakha and Vladimir A. Semionkin, AIP Conf. Proc. **doi: 10.1063/1.4966015**, 020019–1 – 020019–16 (2016).